Dynamic control of the Q factor in a photonic crystal nanocavity

YOSHINORI TANAKA[1], JEREMY UPHAM[1], TAKUSHI NAGASHIMA[1], TOMOAKI SUGIYA[1], TAKASHI ASANO[1] AND SUSUMU NODA[1,2]*

[1]Department of Electronic Science and Engineering, Kyoto University, Kyoto 615-8510, Japan
[2]Photonics and Electronics Science and Engineering Center, Kyoto University, Kyoto 615-8510, Japan
*e-mail: snoda@kuee.kyoto-u.ac.jp

Published online: 2 September 2007; doi:10.1038/nmat1994

High-quality (*Q*) factor photonic-crystal nanocavities[1–8] are currently the focus of much interest because they can strongly confine photons in a tiny space. Nanocavities with ultrahigh *Q* factors of up to 2,000,000 and modal volumes of a cubic wavelength have been realized[8]. If the *Q* factor could be dynamically controlled within the lifetime of a photon, significant advances would be expected in areas of physics and engineering such as the slowing and/or stopping of light[9,10] and quantum-information processing[11,12]. For these applications, the transfer, storage and exchange of photons in nanocavity systems on such a timescale are highly desirable. Here, we present the first demonstration of dynamic control of the *Q* factor, by constructing a system composed of a nanocavity, a waveguide with nonlinear optical response and a photonic-crystal hetero-interface mirror. The *Q* factor of the nanocavity was successfully changed from ∼3,000 to ∼12,000 within picoseconds.

We will first discuss how the *Q* factor of a nanocavity can be controlled dynamically. In general, a photonic-crystal nanocavity is accompanied by a waveguide to introduce (or release) photons into (or from) the nanocavity, as shown schematically in Fig. 1a. In the case of a two-dimensional photonic crystal nanocavity, the *Q* value is determined by two factors: (1) the vertical optical coupling between the nanocavity and free space, and (2) the in-plane optical coupling between the nanocavity and the waveguide. When the individual *Q* factors determined by (1) and (2) are denoted by Q_v and Q_{in}, respectively, the total quality factor (Q_{total}) of the nanocavity can be expressed as $1/Q_{total} = 1/Q_v + 1/Q_{in}$. The value of Q_v is fixed by the structure of the cavity and is mainly determined by the total-internal-reflection-condition for the vertical direction. On the other hand, Q_{in} is determined by the environment of the cavity. For example, when a mirror is placed perpendicular to the waveguide at a specific position as shown in Fig. 1b, Q_{in} is affected by the interaction between the light waves emitted from the nanocavity to the backward direction (solid blue line) and to the forward direction, which are then reflected backward by the mirror (dashed blue line). When this interaction occurs constructively, Q_{in} is reduced. Conversely, Q_{in} is significantly increased when the interference is destructive. The total *Q* factor of the nanocavity is then derived as

$$\frac{1}{Q_{total}} = \frac{1}{Q_{in0}/(1+\cos\theta)} + \frac{1}{Q_v},$$

from coupled-mode theory[13], where θ is the phase difference between the two light waves and Q_{in0} is the in-plane quality factor in the absence of a mirror. If it is assumed that $Q_v \gg Q_{in0}$, Q_{total} can be changed from $Q_{in0}/2$ to Q_v by changing θ from 0 to π. The phase difference can be varied by changing the refractive index of a portion of the waveguide between the nanocavity and the mirror, as shown in Fig. 1b.

Figure 1c shows a concrete example of a system designed for dynamic *Q*-factor control. The nanocavity comprises three missing air holes, and two air holes at the cavity edges are shifted by $0.15a$ to create an electric-field distribution in the form of a gaussian-like function, where a is the lattice constant[1] (see also Fig. 3a). The calculated Q_v of this nanocavity is 55,000. The distance between the cavity and the waveguide is five rows of holes, which gives a Q_{in0} of 3,000. A hetero-interface at one end of the waveguide, formed by a slightly modified lattice constant, acts as a perfect mirror owing to the mode-gap effect[14,15]. The system is assumed to be composed of silicon. The value of θ can be changed by irradiating an optical pulse onto the waveguide to generate free carriers, which reduces the refractive index by the carrier plasma effect. If the duration of the optical pulse is several picoseconds, the refractive index changes on the same timescale. Moreover, in silicon-based photonic crystals, where the carrier lifetime is several nanoseconds[16,17], the refractive-index change can be preserved for a similar length of time, long after the irradiation of the control pulse. If required, further rapid change of the *Q* factor can then be induced by irradiation of another optical pulse.

We use a pump and probe method to demonstrate dynamic control of the *Q* factor using the system shown in Fig. 1c. A pump pulse is irradiated onto the waveguide to change θ, and a probe pulse is sent through the waveguide to the nanocavity to determine changes in the *Q* factor. The intensity and spectrum of the probe pulse emitted from the nanocavity are measured at different times with respect to the arrival of the pump pulse. We assume that the initial θ is approximately zero, which gives the lowest possible Q_{total} of $\sim Q_{in0}/2$, and that the pump pulse changes θ to $\sim\pi$, increasing Q_{total} to its highest possible value of $\sim Q_v$. In addition, the probe pulse duration is chosen to correspond to the photon lifetime in the cavity when Q_{total} is lowest ($= \sim Q_{in0}/2$). In other words, the spectral width of the probe pulse matches the resonant spectrum given by the lowest Q_{total}.

The characteristics of the light emitted from the nanocavity will be strongly dependent on the relative timing of the probe and pump pulses. The three following situations can be visualized. (1) When the probe pulse arrives before the pump pulse, Q_{total} is still at its lowest possible value when the probe pulse interacts

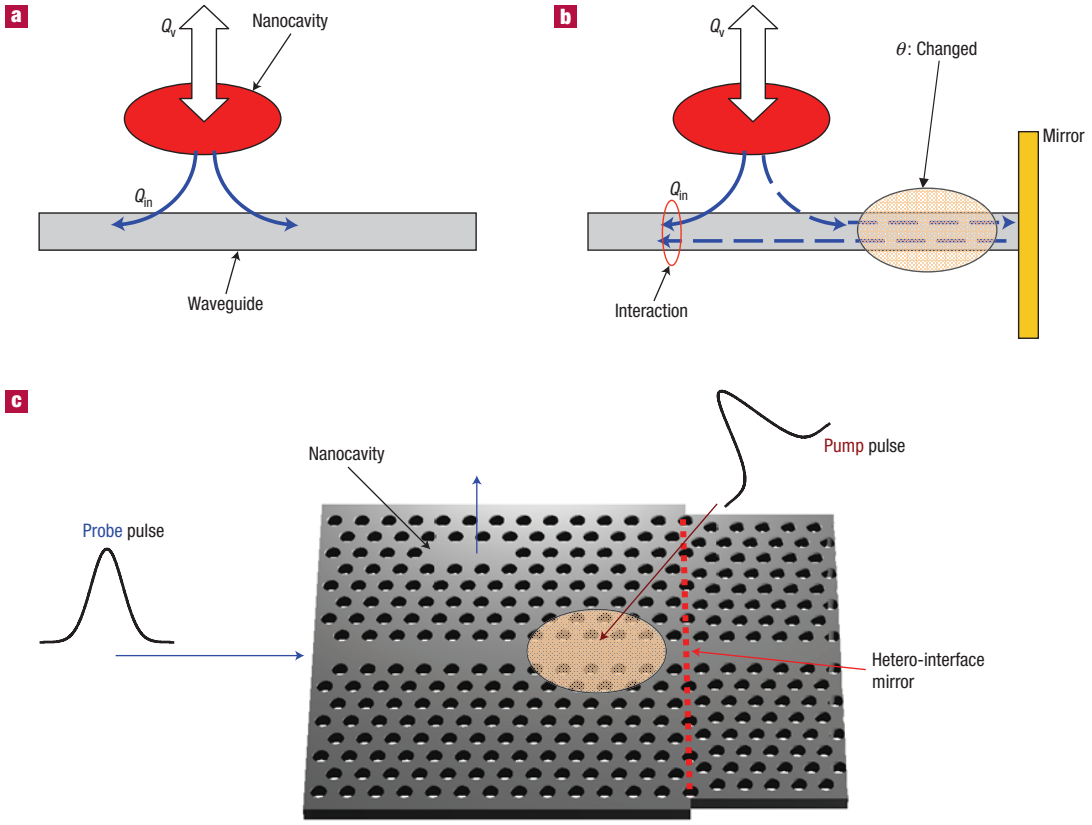

Figure 1 Method for dynamic control of the nanocavity *Q* factor. a, Schematic diagram of the typical configuration of a photonic-crystal nanocavity, where the nanocavity is accompanied by a waveguide which introduces (or releases) photons into (or from) the nanocavity. **b**, Schematic diagram of a system for dynamic control of the *Q* factor, consisting of a cavity, a waveguide with nonlinear optical response (the phase θ is controllable) and a perfect mirror. **c**, Concrete example of such a system. The nanocavity consists of three missing air holes, and air holes at the cavity edges are shifted. A line-defect waveguide is formed in the vicinity of the nanocavity. A hetero-interface, which acts as a perfect mirror, is located at one end of the waveguide, formed by slightly modifying the lattice constant.

with the nanocavity. Although the probe pulse easily couples into the cavity, it also easily leaks back to the waveguide. Thus, only a small number of photons will be emitted from the nanocavity to free space. The spectrum of the emitted light will reflect the lowest Q_{total}. (2) When the probe pulse arrives after the pump pulse, Q_{total} has already reached its highest possible value when the probe pulse arrives. The probe pulse couples weakly to the nanocavity owing to the large spectral mismatch, and almost no emission to free space occurs. (3) When the pump and probe pulses arrive simultaneously, the situation is markedly different to cases (1) and (2). When the probe pulse first reaches the nanocavity, Q_{total} is at its initial value, which enables efficient coupling. The value of Q_{total} is then rapidly increased by the pump pulse, a process that occurs on the same timescale as the probe pulse width. Therefore, the probe pulse trapped by the nanocavity cannot leak out to the in-plane direction, and is instead emitted to the free space; the output power reaches its maximum. The emission spectrum reflects the highest possible value of Q_{total}. In case (3), dynamic change of the Q factor is achieved within the photon lifetime.

The three scenarios above can be modelled quantitatively using the finite-difference time-domain method. Calculations were carried out for various time differences, Δt, between the arrival of the pump and probe pulses, where a negative value denotes that the probe pulse arrives first. The widths of both pulses were set at 4 ps. The pump pulse was assumed to change the refractive index of the waveguide of length $40a$ by -8×10^{-3} within 4 ps, which corresponds to a change of θ from 0 to π, and of Q_{total} from 1,500 to 55,000. Figure 2a shows the radiation power of the probe pulse emitted from the nanocavity to free space as a function of Δt. The vertical radiation is maximal when $\Delta t = 0$ ps (when the two pulses arrive simultaneously). A small amount of radiation is observed when the probe pulse arrives first ($\Delta t < 0$), whereas almost no emission occurs when the pump pulse arrives first ($\Delta t > 0$). Figure 2b–d shows the change in light energy in the nanocavity for three representative cases: $\Delta t = -20$, 0 and 20 ps. When $\Delta t = -20$ ps, the light energy increases rapidly but then quickly falls to zero. When $\Delta t = 20$ ps, the light energy coupled to the nanocavity is always very low. When $\Delta t = 0$ ps, the photon decay time after the probe pulse enters the nanocavity is prolonged, and the photon energy inside the cavity is maintained for much longer than in the other two cases, indicating that a dynamic change of Q_{total} occurs within the photon lifetime. These quantitative results imply that when an ultrafast dynamic change of the Q factor occurs during the pump and probe measurements, both enhancement of the vertically emitted radiation and narrowing of the emission spectrum owing to prolongation of the photon lifetime should be observed.

The results of the above theoretical consideration prompted us to carry out pump and probe experiments using the fabricated sample shown in Fig. 3a, which is designed in the same way as that in Fig. 1c. The pump and probe set-up is shown in Fig. 3b. For the optical pulses we used a mode-locked fibre laser with a pulse

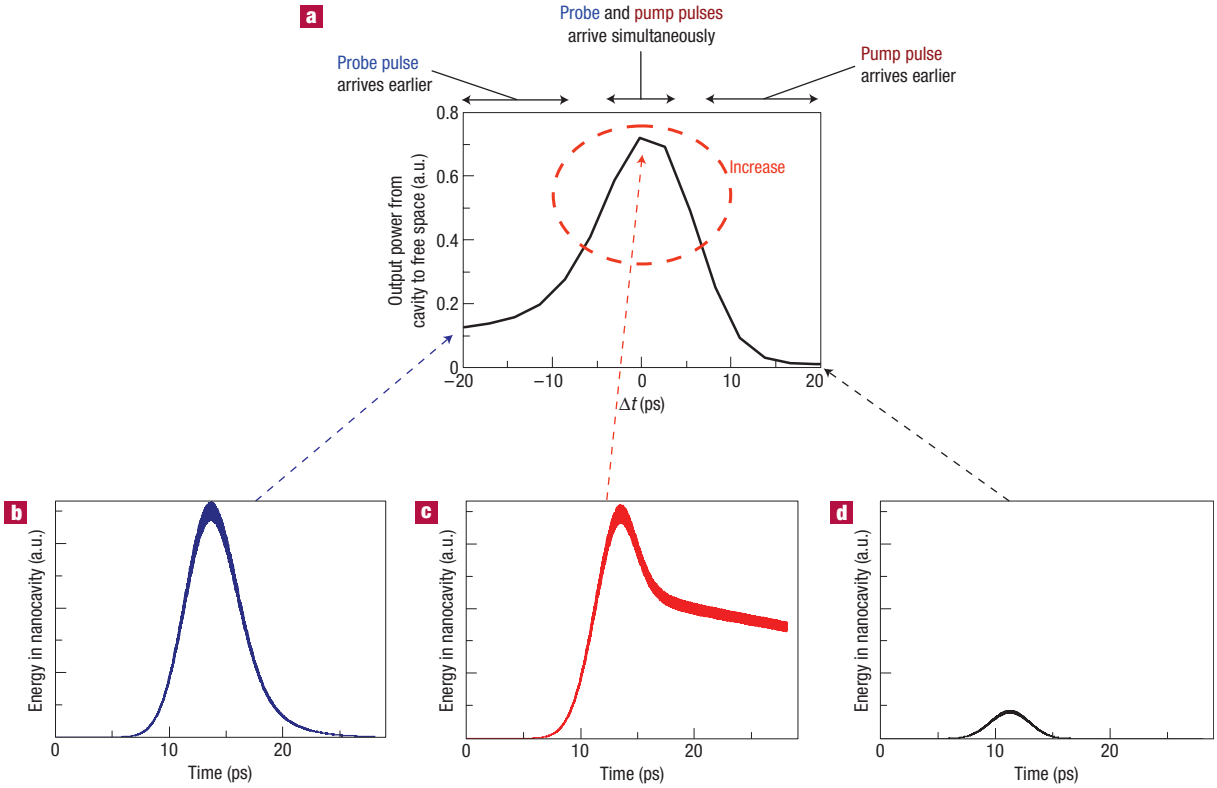

Figure 2 Finite-difference time-domain simulation of pump and probe experiments to demonstrate dynamic change of the *Q* factor. a, Integrated power of the light emitted from the nanocavity to free space as a function of Δt, where Δt represents the time difference between the arrival of the probe and pump pulses. **b–d**, Change of the light energy in the nanocavity for three representative cases: $\Delta t = -20$ (**b**), 0 (**c**) and 20 (**d**) ps.

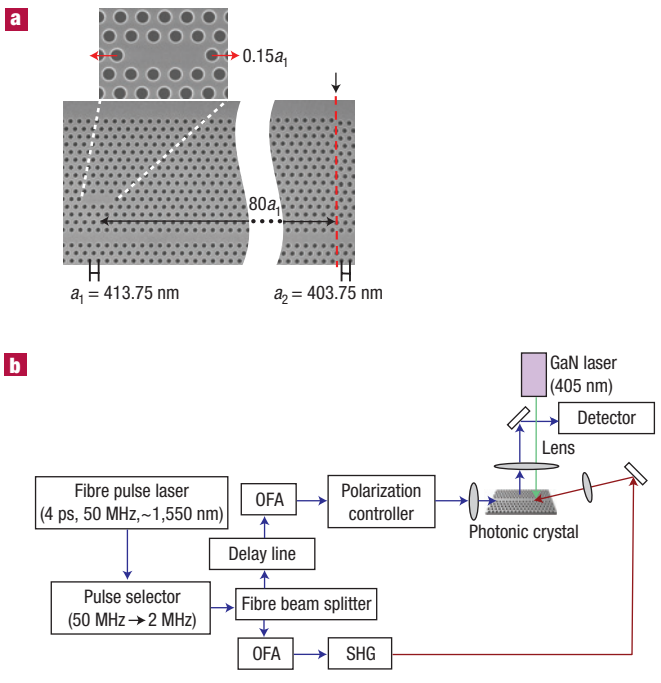

Figure 3 Fabricated sample and experimental set-up. a, Scanning electron micrograph of the fabricated sample. **b**, Schematic diagram of the pump and probe measurement system.

width of ~4 ps and a lasing wavelength of 1.55 μm. This pulse was divided into two. One was passed through a delay line, optical fibre amplifier (OFA) and polarization controller before being injected into the waveguide to act as the probe pulse. The second pulse was passed through an OFA and a second harmonic generator (SHG) and irradiated onto the waveguide to change θ and act as the pump pulse. The wavelength of the pump pulse was set to half (0.775 μm) of the probe pulse wavelength by the SHG. The pump pulse was then absorbed by silicon, enabling free carriers to be generated to change the value of θ. The optical energy of the probe pulse was set to the subpicojoule (pJ) range and that of the pump pulse absorbed by the waveguide to 10–50 pJ, enabling the refractive index change of 10^{-3}–10^{-2} necessary to change θ by ~π. In the set-up shown in Fig. 3b, a continuous-wave GaN laser was used to fine-tune the initial value of θ as close to zero as possible by thermal effects. A delay line applied to the probe pulse was used to control the timing between the probe and pump pulses.

The integrated output power for the probe pulse emitted from the nanocavity as a function of Δt is shown in Fig. 4a. The pump pulse energy absorbed by the waveguide was set at 23 pJ, which induces a change of θ by π. When the probe pulse arrived before the pump pulse, some amount of output power was observed. On the other hand, when the probe pulse arrived after the pump pulse, much less output power was observed from the nanocavity, in good agreement with the theoretical calculations. The most important point in Fig. 4a is that when the probe and pump pulses arrived simultaneously, the output power clearly increased with respect to the other two cases. We note that when the pump pulse energy was varied to give phase shifts other than ~π, no increase was observed.

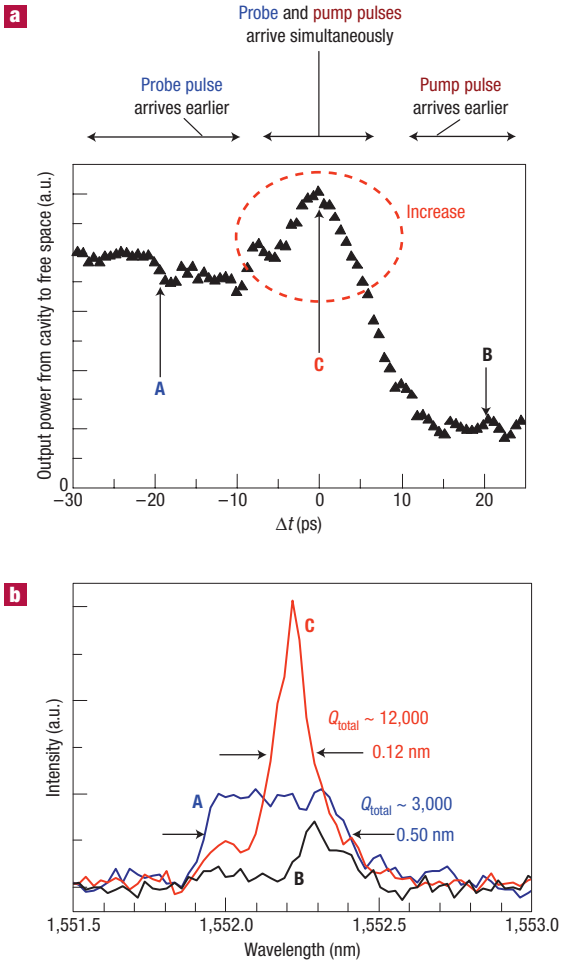

Figure 4 Experimental results of pump and probe measurements of the dynamic change of the *Q* factor. a, Integrated power of the probe pulse emitted from the cavity to free space as a function of Δt. **b**, Spectra of the emitted light for three representative cases: **A** $\Delta t = -20$ ps, **B** $\Delta t = 20$ ps and **C** $\Delta t = 0$ ps.

Therefore, the increase of output power for $\Delta t = 0$ ps indicates that the Q factor was changed within 4 ps by the interaction between the probe and pump pulses. To confirm this observation, we measured the emitted probe pulse spectra for various values of Δt, as shown in Fig. 4b. When the pump pulse arrived 20 ps before the probe pulse (arrow (B) in Fig. 4a), the output power was too low to estimate the linewidth of the emission spectrum accurately. When the probe pulse arrived 20 ps before the pump pulse (arrow (A) in Fig. 4a), the output spectrum was rather broad with an estimated linewidth of ~0.50 nm, which corresponds to a Q factor of ~3,000. When the probe and pump pulses arrived simultaneously (arrow (C) in Fig. 4a), the resonant spectrum was sharper with a linewidth of ~0.12 nm, corresponding to a Q factor of ~12,000. When compared with the theoretical analysis described above, the experimental results for $\Delta t = 0$ clearly indicate that we have achieved dynamic control of the Q factor (from ~3,000 to ~12,000) on a picosecond timescale.

Finally, we make a more quantitative comparison between the experimental and theoretical results shown in Figs 2a and 4a. The power of the emitted light for $\Delta t = 0$ ps was calculated to be approximately six times that for $\Delta t = -20$ ps, whereas in the corresponding experiment, the power increased by a factor of 1.5. One possible reason for this quantitative difference may be the absorption of light by free carriers in the waveguide region where the pump pulse was injected. The destructive interference between the two light waves (solid and dashed blue lines in Fig. 1b) would then be incomplete, allowing light to escape from the nanocavity in the in-plane direction. If the pump pulse photon energy could be reduced and excess heating of the carriers and phonons suppressed, then free-carrier absorption might be reduced, and a much greater increase in emission power would be expected.

In summary, we have successfully demonstrated the dynamic change of the Q factor of a nanocavity from ~3,000 to ~12,000 on a picosecond timescale by using a system composed of a nanocavity, a waveguide with nonlinear response and a hetero-interface mirror. We believe that this demonstration is an important step towards realization of the slowing and/or stopping of light, and quantum-information processing where nanocavities could be integrated on a chip and the transfer, storage and exchange of photons would be possible through integrated waveguides.

Received 25 June 2007; accepted 30 July 2007; published 2 September 2007.

References

1. Akahane, Y., Asano, T., Song, B. S. & Noda, S. High-*Q* photonic nanocavity in a two-dimensional photonic crystal. *Nature* **425**, 944–947 (2003).
2. Song, B. S., Noda, S., Asano, T. & Akahane, Y. Ultra-high-*Q* photonic double-heterostructure nanocavity. *Nature Mater.* **4**, 207–210 (2005).
3. Asano, T., Song, B. S., Akahane, Y. & Noda, S. Ultrahigh-*Q* nanocavities in two-dimensional photonic crystal slabs. *IEEE J. Select. Top. Quant. Electron.* **12**, 1123–1134 (2006).
4. Kuramochi, E. *et al.* Ultrahigh-*Q* photonic crystal nanocavities realized by the local width modulation of a line defect. *Appl. Phys. Lett.* **88**, 041112 (2006).
5. Srinivasan, K., Barclay, P. E. & Painter, O. Fabrication-tolerant high quality factor photonic crystal microcavities. *Opt. Express* **12**, 1458–1463 (2004).
6. Yoshie, T. *et al.* Vacuum Rabi splitting with a single quantum dot in a photonic crystal nanocavity. *Nature* **432**, 200–203 (2004).
7. Noda, S. Seeking the ultimate nanolaser. *Science* **314**, 260–261 (2006).
8. Noda, S., Fujita, M. & Asano, T. Spontaneous-emission control by photonic crystals and nanocavities. *Nature Photon.* **1**, 449–458 (2007).
9. Yanik, M. F. & Fan, S. Stopping light all optically. *Phys. Rev. Lett.* **92**, 083901 (2004).
10. Tanaka, Y., Asano, T. & Noda, S. *The Pacific Rim Conference on Lasers and Electro-Optics (CLEO/PR) 2005, CWE4-3, Tokyo, Japan, July 11–15* 1024–1025 (2005).
11. Hartmann, J. H., Brandao, F. G. S. L. & Plenio, M. B. Strongly interacting polaritons in coupled arrays of cavities. *Nature Phys.* **2**, 849–855 (2006).
12. Hennessy, K. *et al.* Quantum nature of a strongly coupled single quantum dot–cavity system. *Nature* **445**, 896–899 (2007).
13. Manolatou, C. *et al.* Coupling of modes analysis of resonant channel add–drop filters. *IEEE J. Quant. Electron.* **35**, 1322–1331 (1999).
14. Song, B. S., Noda, S. & Asano, T. Photonic devices based on in-plane hetero photonic crystals. *Science* **300**, 1537 (2003).
15. Song, B. S., Asano, T., Akahane, Y., Tanaka, Y. & Noda, S. Transmission and reflection characteristics of in-plane hetero-photonic crystals. *Appl. Phys. Lett.* **85**, 4591–4593 (2004).
16. Barclay, P. E., Srinivasan, K. & Painter, O. Nonlinear response of silicon photonic crystal microresonators excited via an integrated waveguide and fiber taper. *Opt. Express* **13**, 801–820 (2005).
17. Almeida, V. R., Barrios, C. A., Panepucci, R. R. & Lipson, M. All-optical control of light on a silicon chip. *Nature* **431**, 1081–1084 (2004).

Acknowledgements

This work was supported by Research Programs (Grant-in-Aid, COE, and Special Coordination Fund) for Scientific Research from the Ministry of Education, Culture, Sports, Science and Technology of Japan, and also by Core Research for Evolutional Science and Technology of the Japan Science and Technology Agency.
Correspondence and requests for materials should be addressed to S.N.

Competing financial interests

The authors declare no competing financial interests.